Journal of Quantitative Spectroscopy & Radiative Transfer 278 (2022) 108001

Contents lists available at ScienceDirect

Journal of Quantitative Spectroscopy & Radiative Transfer

journal homepage: www.elsevier.com/locate/jqsrt

Molecular oxygen fine structure with sub-kHz accuracy

M.A. Koshelev*, G.Yu. Golubiatnikov, I.N. Vilkov, M.Yu. Tretyakov

Institute of Applied Physics, Russian Academy of Sciences, 46 Ulyanov str., Nizhny Novgorod 603950, Russia

ARTICLE INFO

Article history:
Received 22 October 2021
Revised 12 November 2021
Accepted 14 November 2021
Available online 17 November 2021

ABSTRACT

Two spectrometers with complementary capabilities, in particular, a spectrometer with radioacoustic detection of absorption and a conventional video spectrometer, were used for systematic measurement of the frequencies of all magnetic-dipole transitions of the fine structure of the $^{16}O^{16}O$ molecule in the ground state $X^3\Sigma_g^-$ up to rotational states with $N = 43$. The obtained data set made it possible to refine significantly (the uncertainty was reduced from 4 to 6 times) the molecular constants responsible for the fine structure of the rotational oxygen levels, and to reduce the uncertainty in predicting the frequencies of the corresponding transitions by about an order of magnitude. For all fine-structure lines essential for atmospheric applications, the uncertainty is less than 1 kHz.

Introduction

Molecular oxygen is one of the main components of the Earth's atmosphere; therefore, the most intense part of O_2 spectrum has been studied quite well in various frequency ranges from microwave to ultraviolet. Repeated measurements in order to refine the parameters of lines related to the microwave range, in particular, the oxygen absorption band at 60 GHz, have a long history [1–16]. In one of the latest papers [16], devoted to the measurements of the positions of oxygen lines located from the microwave to the THz range, the most complete analysis of experimental data for various isotopologues both in the ground and in the excited electronic state of the oxygen molecule is presented. Nevertheless, at present, there remains a need for precision measurements of the oxygen line parameters, since, due to the uniform distribution of O_2 molecules in the atmosphere, their lines are very convenient for remote sensing and, in particular, for reconstructing the temperature profile [17–19] or the surface pressure [20]. Conventional microwave radiometric systems use a band of magnetic fine structure transitions of $^{16}O^{16}O$ in the ground vibrational and electron state $X^3\Sigma_g^-$ located near 60 GHz [21–23].

Modern precision laboratory studies of the shape of individual resonance lines with a high signal-to-noise ratio make it possible to determine the line parameters with high accuracy, including those responsible for such subtle effects as collisional line narrowing (Dicke effect) [24] and the dependence of collisional relaxation on the velocity of molecules – "wind effect" [25]; these effects are used in propagation models. For a thorough understanding of the O_2 spectrum required for accurate atmospheric absorption modeling, it is important to have a complete idea of the spectrum and to know how fully and accurately existing models can reproduce the spectrum. Therefore, the study of previously unobserved low-intensity lines, for example, electro-quadrupole transitions [26] or purely rotational transitions with high quantum numbers [27] is of interest, despite the fact that the parameters of these lines are rather well predicted theoretically and their further improvement is not of direct relevance for the detection of O_2 in the atmosphere. In this regard, and within the framework of improving spectroscopic parameters of the 60-GHz band of atmospheric O_2, it is interesting to estimate (i) the accuracy of the extrapolation of known positions of the fine-structure lines on the lines with the larger quantum number of the total angular momentum J based on the currently known values of the effective molecular constants and (ii) what extent this accuracy can be increased to using the capabilities of modern microwave spectrometers.

For this purpose, systematic measurements of the line positions were carried out in both series of transitions $N^- = (N, J = N)$–$(N J = N–1)$ and $N^+ = (N, J = N)$–$(N, J = N+1)$, constituting the fine structure band of the oxygen molecule $^{16}O_2$, using a spectrometer with radio-acoustic detection of absorption (RAD spectrometer, see [28,29] and references therein) and a direct absorption spectrometer (video spectrometer) [30,31], including previously unobserved low-intensity transitions.

Until now, the frequencies of the fine structure transitions of O_2 were measured for lines with the maximum value of the quantum number of the orbital angular momentum $N = 39$, while the frequencies of some lines with lower N were not experimentally

* Corresponding author.
E-mail address: koma@ipfran.ru (M.A. Koshelev).

https://doi.org/10.1016/j.jqsrt.2021.108001
0022-4073/

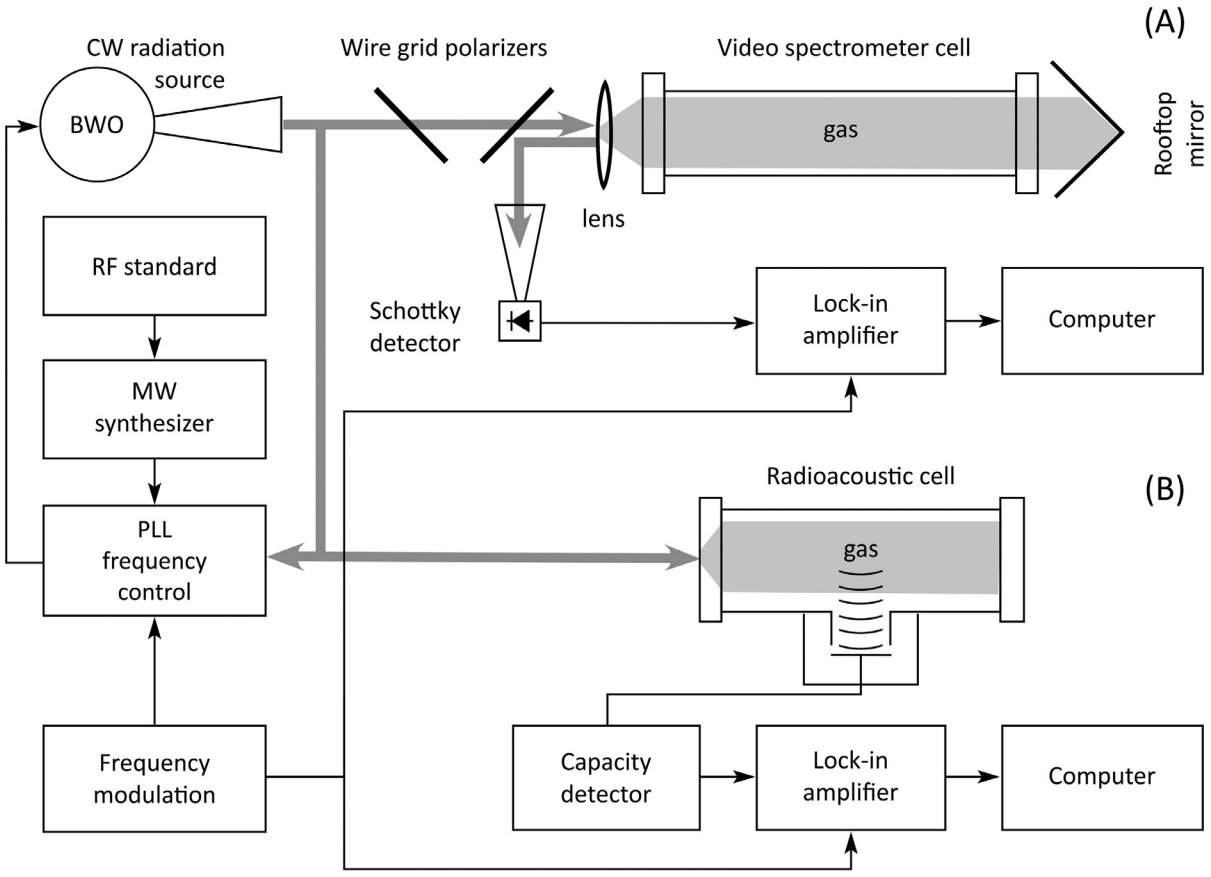

Fig. 1. Block diagram of the experiment.

determined. In this paper, we measure the frequencies of all fine structure lines of oxygen up to $N = 43$. For 9 transitions, including 43^+ and 43^-, the peak absorption of which is about 10^{-10} cm^{-1}, the frequencies were measured for the first time.

The data analysis was carried out on the basis of effective molecular constants using the SPFIT program [32], as well as in [16], and with a set of measured frequencies of rotational transitions recommended by the Cologne Database for Molecular Spectroscopy (CDMS) [33], the information from which is used as the most accurate previous data for comparison with the results obtained. The molecular constants of the fine structure obtained as a result of our work have several times less statistical uncertainty and provide about an order of magnitude more accurate prediction of the frequencies of the corresponding transitions.

Experiment

A detailed description of the spectrometers used for recording the lines of the oxygen fine structure is presented in [28,29] and references therein and in [30,31] for the RAD and video spectrometers, respectively. The combined block diagram of the setups is shown in Fig. 1. Backward-wave oscillators (OB-69 and OB-70 for the 60-GHz band and OB-71 for the 118-GHz line) stabilized using a phase-locked loop (PLL) system against a highly stable signal from the reference synthesizer Anritsu MG3692C were used as a radiation source in both spectrometers. The radiation frequency was modulated inside the PLL using a Tektronix AFG3101 arbitrary radiofrequency waveform generator. A 10-MHz signal from the GPS time and frequency system FS740 (Stanford Research) was used as a reference for the synthesizer and modulating generator allowing the frequency uncertainty of about 10^{-13}. In the video spectrometer, the radiation was recorded by a crystal detector with further demodulation by a lock-in amplifier. Most spectra were recorded at room temperature. For recording spectral lines, both instruments used the method of radiation frequency modulation (sinusoidal) with a known deviation, followed by a synchronous detection of the signal at the second harmonic of the modulation frequency [34]. This method significantly reduces the parasitic baseline perturbing the shape of the line under study. Note that careful alignment of the radiation beam relative to the cell and mechanical stability of the radiation path helps to reduce the baseline influence more efficiently than reduction of the radiation power in both instruments.

To exclude the influence of external magnetic fields on the shape of the oxygen magnetic-dipole lines, the RAD spectrometer cell, manufactured mainly of non-magnetic materials (copper and stainless steel), was demagnetized and placed inside a double permalloy shield. The cell sensitivity decreases with decreasing gas pressure below 1 Torr [28]; therefore, the operating pressure value was chosen as a compromise between narrow lines (low pressures) and the spectrum quality (high signal-to-noise ratio (SNR)). Both factors improve the accuracy of determining the line center frequency. The pressure was 0.15–0.3 Torr and 1 Torr (the maximum of the cell sensitivity) for the most intense and less intense transitions, respectively. Under these conditions, the spectral resolution of the spectrometer is limited by the collisional linewidth constituted up to several megahertz. However, previous studies have shown (see, e.g., [35]) that the position of the line center can be determined using the RAD spectrometer with an accuracy of the order of 1 kHz. Such high accuracy is ensured by (i) the high SNR on the line recording, (ii) choosing an adequate line profile model, and (iii) multiple measurements with system-

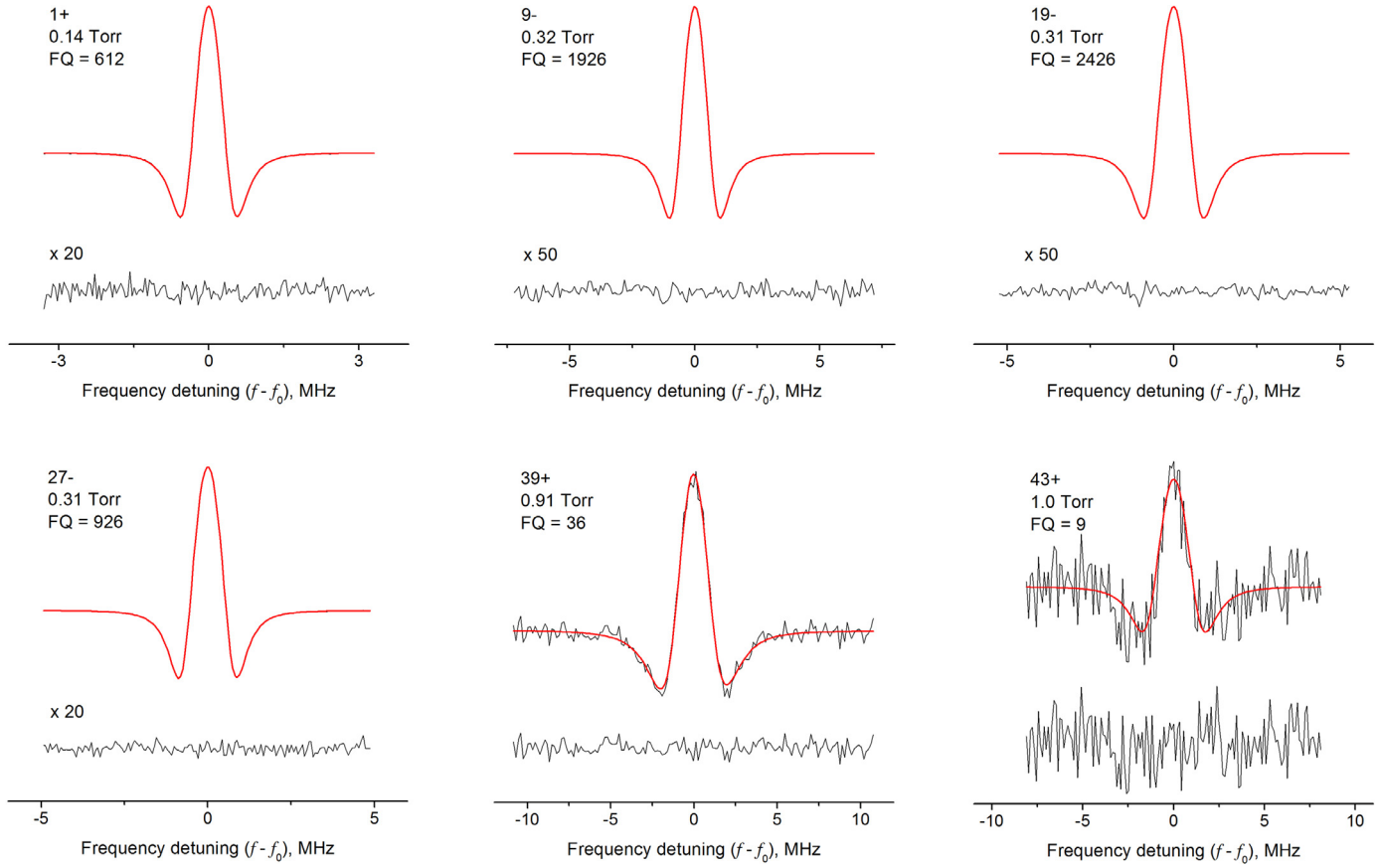

Fig. 2. Examples of the line recording obtained with the RAD spectrometer. FQ – fit quality. Scaling factors (if different from 1) are presented for each residual.

atic variation of the spectrometer baseline. However, simultaneous measurements with video spectrometer operating at significantly lower pressures can identify and minimize potential systematic errors [30]. In the framework of this work, we used the complementary capabilities of both these spectrometers.

The cylindrical cell of the video spectrometer (2 m long, inner diameter 11 cm), like the RAD cell, had a magnetic shielding (wrapped with a permalloy tape in several layers). A double pass configuration was used which is also applied in this spectrometer to observe the Lamb dip [31]. However, due to the small magnetic dipole moment of the oxygen molecule, about 2 Bohr magnetons (which corresponds to an electric dipole of only 0.018 D) and the low intensity of the lines (a peak absorption is less than 10^{-6} cm^{-1}), it was impossible to observe the manifestation of the transition saturation (Lamb dip) with the available radiation sources. Therefore, the spectral resolution in the measurements was limited by the Doppler linewidth ($\sim$ 120 kHz) at a gas pressure of 20–30 mTorr.

Examples of line recordings obtained with the RAD spectrometer are shown in Fig. 2. The analysis of the observed line shape was carried out by the corresponding model function, constructed on the basis of the generally accepted spectral line profiles (Lorentz or Voigt), taking into account the type of modulation and demodulation used [34]. The statistical error of the line center determining resulted from the fit of the RAD spectrometer recordings was less than 1 kHz and more than 100 kHz for strong (SNR $>$ 1000) and the weakest lines ($N = 43$ with SNR $\sim$ 7), respectively (Table 1).

In any spectrometer, one of the major sources of error in determining the spectral line shape parameters, and, first of all, the central frequency, are standing waves in the spectrometer waveguide path (the so-called etaloning). To reduce this error, several line recordings were obtained with the RAD spectrometer at different positions of the gas cell relative to the radiation source (4–10 positions). The final frequency of the line center was determined by the averaging of the obtained values. Typical scatter of the measured values of the line center relative to its mean value was comparable with the statistical error for most of the lines studied.

For six fine structure lines ($N = 1^-$, 1^+, 7^+, 11^+, 15^+, and 19^-), the line positions were studied at different pressures and temperatures in the range 0.2–2.5 Torr and from –39 to + 85 C, respectively (a detailed analysis of the results of this study will be published separately, together with the temperature dependences of the speed dependent broadening). Additionally, experimental data from [29] were used. This allowed estimating the pressure shift of the central frequency of the oxygen fine structure transitions. The results of this study for the lines $N = 1^+$, 11^+, and 19^- (as typical examples) are shown in Fig. 3.

At each temperature, the line was recorded at several pressures (6–8 points) and several positions of the cell relative to the radiation source. The observed variations of the line center demonstrated the expected linear dependence on pressure and did not reveal a notable temperature dependence. Therefore, all temperature points were used simultaneously to analyze the shifting effect. Fig. 3 shows that the observed frequency of the line center, on average, systematically increases with increasing pressure, and the displacement normalized to pressure increases with increasing rotational quantum number N. This behavior was observed for all lines studied. The obtained shifting coefficients of the line centers are collected in Fig. 4. In addition to the six points corresponding to our detailed studies (shown by filled circles), Fig. 4 shows data

Table 1
Measured and calculated using the derived constants (Table 3) frequencies of the oxygen $^{16}O_2$ fine structure transitions in MHz.

Line notation, *N*	Observed			Calculated
	RAD		Video	
	Measured	Corrected		
1^-	118,750.3328(8)	118,750.3325(8)	118,750.339(3)	118,750.3328(5)
1^+	56,264.7765(25)	56,264.7762(23)	56,264.781(5)	56,264.7738(3)
3^-	62,486.2519(3)	62,486.2509(4)	62,486.267(5)	62,486.2520(3)
3^+	58,446.5897(8)	58,446.5893(8)	58,446.588(5)	58,446.5883(3)
5^-	60,306.0558(9)	60,306.0553(9)	60,306.056(5)	60,306.0547(3)
5^+	59,590.9829(11)	59,590.9825(11)	59,590.996(5)	59,590.9829(3)
7^-	59,164.2042(17)	59,164.2036(17)	59,164.205(5)	59,164.2019(3)
7^+	60,434.7781(26)	60,434.7776(26)	60,434.780(5)	60,434.7779(3)
9^-	58,323.8766(17)	58,323.8759(17)	58,323.880(5)	58,323.8740(4)
9^+	61,150.5628(14)	61,150.5622(15)	61,150.568(5)	61,150.5620(3)
11^-	57,612.4834(5)	57,612.4825(11)	57,612.486(5)	57,612.4828(4)
11^+	61,800.1577(7)	61,800.1570(7)	61,800.159(5)	61,800.1575(3)
13^-	56,968.2077(15)	56,968.2067(15)	56,968.209(5)	56,968.2076(4)
13^+	62,411.2209(16)	62,411.2199(15)	62,411.221(5)	62,411.2193(3)
15^-	56,363.3983(16)	56,363.3966(12)	56,363.399(5)	56,363.3944(5)
15^+	62,997.9828(4)	62,997.9818(4)	62,997.981(5)	62,997.9818(3)
17^-	55,783.8155(51)	55,783.8134(43)	55,783.808(5)	55,783.8105(5)
17^+	63,568.5235(7)	63,568.5221(12)	63,568.527(5)	63,568.5231(3)
19^-	55,221.3812(21)	55,221.3793(26)	55,221.375(5)	55,221.3796(6)
19^+	64,127.7770(16)	64,127.7738(18)	64,127.770(5)	64,127.7713(4)
21^-	54,671.1772(33)	54,671.1750(32)	54,671.176(5)	54,671.1754(6)
21^+	64,678.9103(27)	64,678.9066(28)	64,678.914(5)	64,678.9062(5)
23^-	54,130.0229(22)	54,130.0204(19)	54,130.021(5)	54,130.0204(7)
23^+	65,224.0761(22)	65,224.0717(25)	65,224.073(5)	65,224.0729(6)
25^-	53,595.7724(13)	53,595.7697(12)	53,595.773(5)	53,595.7720(7)
25^+	65,764.7754(11)	65,764.7703(17)	65,764.775(5)	65,764.7729(7)
27^-	53,066.9352(10)	53,066.9319(23)	53,066.934(5)	53,066.9313(8)
27^+	66,302.0959(25)	66,302.0902(29)	66,302.096(5)	66,302.0900(8)
29^-	52,542.4208(54)	52,542.4157(35)	52,542.416(5)	52,542.4174(9)
29^+	66,836.8298(16)	66,836.8247(17)	66,836.840(5)	66,836.8275(9)
31^-	52,021.4379(63)	52,021.4304(59)	52,021.430(5)	52,021.4303(11)
31^+	67,369.6009(61)	67,369.5940(38)	67,369.611(5)	67,369.5942(12)
33^-	51,503.3844(74)	51,503.3748(77)	51,503.369(5)	51,503.3641(15)
33^+	67,900.8658(74)	67,900.8563(81)	67,900.870(5)	67,900.8615(17)
35^-	50,987.7578(123)	50,987.7501(120)	50,987.750(10)	50,987.7513(22)
35^+	68,431.0119(94)	68,431.0009(73)	68,431.004(10)	68,431.0005(24)
37^-	50,474.2385(36)	50,474.2273(46)	50,474.220(10)	50,474.2245(31)
37^+	68,960.339(19)	68,960.323(15)	68,960.312(5)	68,960.3086(35)
39^-	49,962.493(36)	49,962.481(36)	–	49,962.4904(44)
39^+	69,489.050(43)	69,489.048(36)	–	69,489.0275(50)
41^-	49,452.336(56)	49,452.322(56)	–	49,452.3115(62)
41^+	70,017.372(38)	70,017.356(38)	–	70,017.3563(69)
43^-	48,943.607(149)	48,943.589(149)	–	48,943.4932(84)
43^+	70,545.455(72)	70,545.436(70)	–	70,545.4613(94)

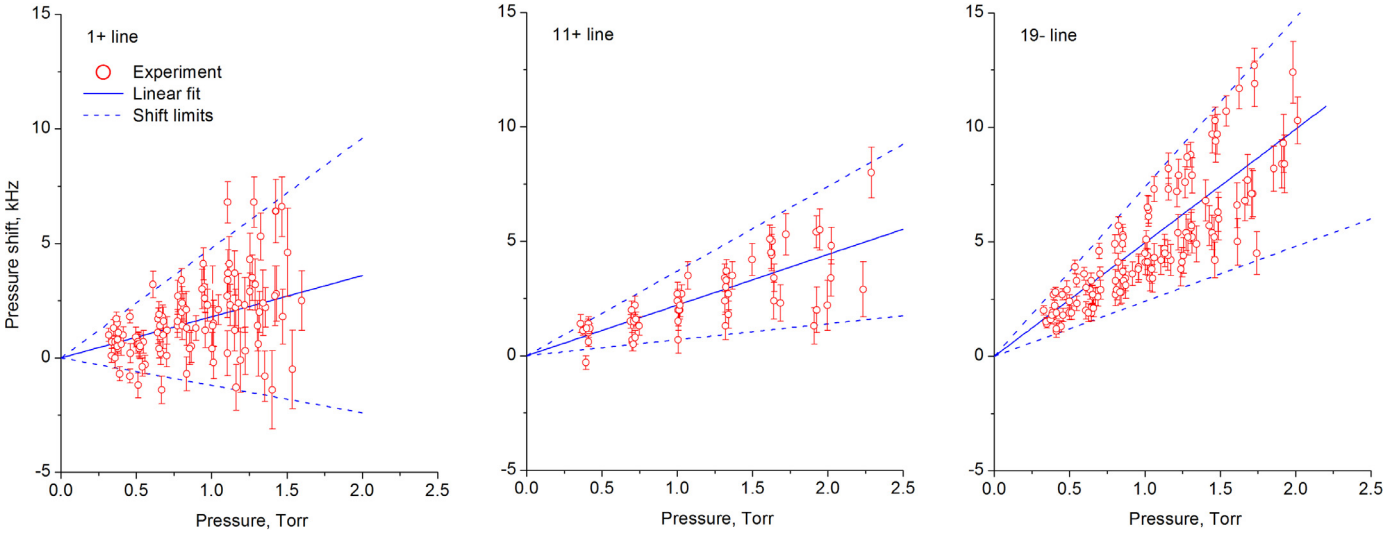

Fig. 3. Line center position observed at different pressures (see text for details).

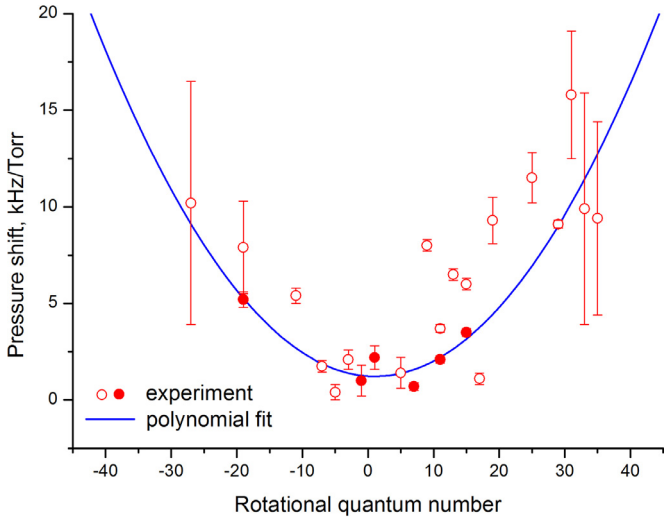

Fig. 4. Pressure shift coefficient of the line center as a function of rotational quantum number. Circles are experimental values; solid line is a second-order polynomial fit.

from [29] for other lines (unshaded circles), which are less accurate and reliable, but, nevertheless, they generally confirm the observed dependence.

It was noted in our previous studies of the oxygen fine structure lines [15,29], that due to the weakness of the pressure shifting effect, it was only possible to estimate from the experimental data that the effect does not exceed ±15 kHz/Torr for all previously observed lines of the 60-GHz band and ±4.5 kHz/Torr for the 1^- line. New data significantly improve this estimate, making it possible, in particular, to consider the magnitude of the effect as a function of the rotational quantum number.

It should be noted that although all said above looks like a manifestation of the well-known collisional effect [36], which must be taken into account when determining the frequencies of molecular transitions unshifted by pressure, the nature of the observed effect may be different. Residual permanent magnetic fields can be in the gas cell (despite double screening and careful demagnetization of metallic elements), leading to the line splitting into two groups of Zeeman components, the number of them rapidly increases with N. The components are arranged symmetrically relative to the position of the unsplit line center, but the amplitudes of the corresponding symmetric components may differ in the presence of a circularly polarized component of the probe radiation [37]. The latter can arise due to parasitic reflections in the oversized waveguide part of the gas cell, despite the fact that the initial BWO radiation is linearly polarized. A detailed analysis of the nature of the observed displacement of the oxygen line positions will be performed in our further works, and in this study, we only use the experimentally obtained information (Fig. 4) to determine the pressure-unshifted frequencies of the fine structure transitions. These frequencies we used for further analysis, however, for completeness, we present measured frequencies before and after correction in Table 1. Errors indicated in Table 1 for the RAD spectrometer data are a combination of (i) a statistical error, determined by the signal-to-noise ratio, (ii) the spread of the frequency values obtained at different relative positions of the cell and the radiation source, and (iii) errors in determining the line shift (for the second column).

Typical examples of line recordings obtained using video spectrometer are shown in Fig. 5. It turned out from the data analysis that the error in determining the central frequencies is ±5 kHz for most of the lines. This is somewhat worse than the RAD spectrometer uncertainties, despite the lines recorded using the video spectrometer were an order of magnitude narrower. It is caused by a much stronger correlation between the parameters of the line shape and the baseline in the model function of the video spectrometer in comparison with that of the RAD spectrometer. In cases where the baseline significantly exceeded the signal from the spectral line (see, for example, the line 35^+ in Fig. 5), the degree of the fitting polynomial responsible for describing the baseline in the model function had to be increased to the 4th, which increased the total number of the model variable parameters and the correlation between them. The spread of the line center frequency values determined for the repeated recordings reached in some cases 10% of the line width, while the statistical error was less than 1% of the line width. Therefore, the errors of the frequencies measured using the video spectrometer (Table 1) are mainly determined by the baseline models used. The sensitivity of the video spectrometer was determined by the signal accumulation time and did not exceed 10^{-9} cm^{-1}. Line measurements with this spectrometer were performed up to $N = 37$.

Data analysis

The SPFIT program [32] is used to calculate the parameters of the effective Hamiltonian of the ground vibrational and electronic state $X^3\Sigma_g^-$ which also takes into account the rotation of the oxygen molecule, the splitting of the rotational levels due to the molecular spin ($S = 1$), the spin-rotational interaction including two correction terms responsible for centrifugal distortion and nonparabolicity of the potential. Similar to previous papers [14–16], ten adjustable spectroscopic constants are used for fitting, which make it possible to carry out a comparative analysis of the previous data and the results of our new measurements. The obtained frequencies of the fine structure transitions are fitted simultaneously with the rotational transition frequencies obtained on the basis of the experiment and tabulated in the database of the Cologne University [33]; these rotational frequencies are currently considered to be the most reliable.

At first, we analyze the deviation of our two experimental sets of frequencies from the expected smooth dependence on the rotational quantum number N. For comparison, a similar check is performed for the frequencies of the fine structure lines from the previous papers [14,33]. For an adequate comparison, all datasets are supplemented with frequencies of the missing fine structure lines (from the most complete set of data of the RAD spectrometer from Table 1) and the same set of rotational lines. Thus, in all cases, the model with 10 variable parameters is fitted to the frequencies of 62 lines, but a comparison is made only in the range of quantum numbers of the initial data.

Fig. 6 shows the dependence of the standard deviation of (obs.–calc.) frequencies of the fine structure lines for different datasets; the deviation is calculated for the lines with quantum numbers from 1 to N_{max} depending on N_{max}. The video spectrometer data have approximately the same scatter as the most accurate previous data [33] (which almost coincide with the experimental frequencies of the fine structure lines from [15], supplemented with the results of measurements of 8 lines with large N from [6]), and the scatter of the RAD spectrometer data is up to 3 times less. The advantages of these three datasets over the earlier dataset of Golubiatnikov et al. [14] are obvious. These three sets have comparable accuracy and will be used in subsequent stages of the analysis as the results of equivalent independent experimental studies.

In the next step, we try to reveal possible systematic differences between the selected three datasets. For this, the model parameters are optimized by the SPFIT program simultaneously to all three datasets (total 140 values of the frequencies of 62 transitions). The deviations of the experimental frequencies of the fine

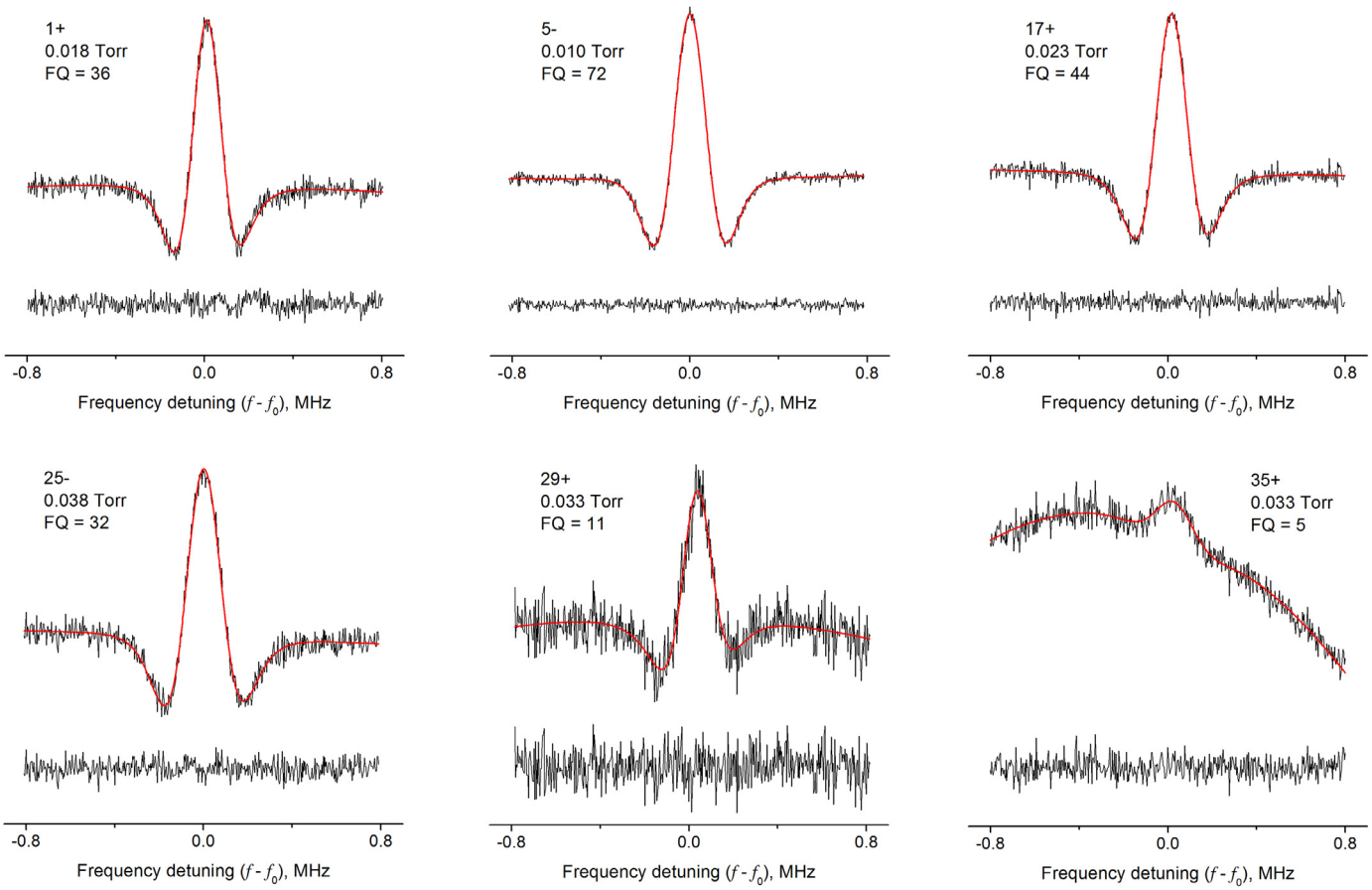

Fig. 5. Examples of line recordings obtained with the video spectrometer.

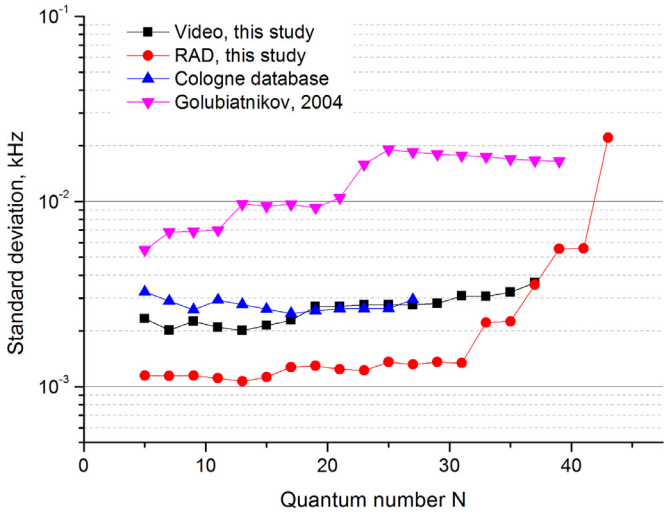

Fig. 6. Standard deviation of experimental frequencies from a calculated dependence as a function of N_{max} for different datasets.

structure transitions from the optimization result are shown in Fig. 7. All sets agree with each other within the combined experimental error. The exception is the lines (33^-, 19^-, 1^-, 29^+, and 31^+), for which the discrepancy between the measurement results in one of the three series exceeds the measurement error. All presented data are, on average, shifted towards positive deviations; the average deviation is 2.4 kHz. At first glance, this seems strange, but it is explained by the fact that the optimization process also takes into account frequencies of 15 rotational transitions, which will be discussed below.

The average deviation of the experimental points of different series from the calculation result is estimated similarly to the analysis of data smoothness as a function of the maximum rotational number N_{max} (Fig. 6), since the frequencies of the low-intensity lines at the edges of the band have a larger uncertainty. This result is shown in Fig. 8.

Fig. 8 allows quantitative estimates of the systematic mean bias of one dataset from another. The increase in the difference between the data of [15] and the new RAD spectrometer measurements with the increase in the quantum number can probably be explained by neglecting the pressure shifting of the line frequency, since in [15] the measurements were carried out at approximately the same pressures. The mean deviation between the sets of frequencies obtained in this work using RAD (with shifting correction) and video spectrometers (at pressures when the shift is negligible) is 2–4 kHz and has no explanation. It should be noted, however, that this deviation is close to the RMS of the frequency spread for this dataset (~3 kHz, Fig. 3) and less than the measurement error (5–10 kHz, Table 1).

At the next step, we analyze the influence of the new data on the accuracy of the description of oxygen rotational transitions. The experimental frequencies of these transitions can be found in the following sources. The work [7] reports the first measurement of five lines in the range from 0.77 to 2.5 THz using the tunable sideband to the differential frequency of two CO_2 lasers. In the subsequent work [9], the same spectrometer was used to re-measure the line frequency at 2.5 THz and for the first measurement of the line at 1.5 THz. The first microwave measurements of the frequencies

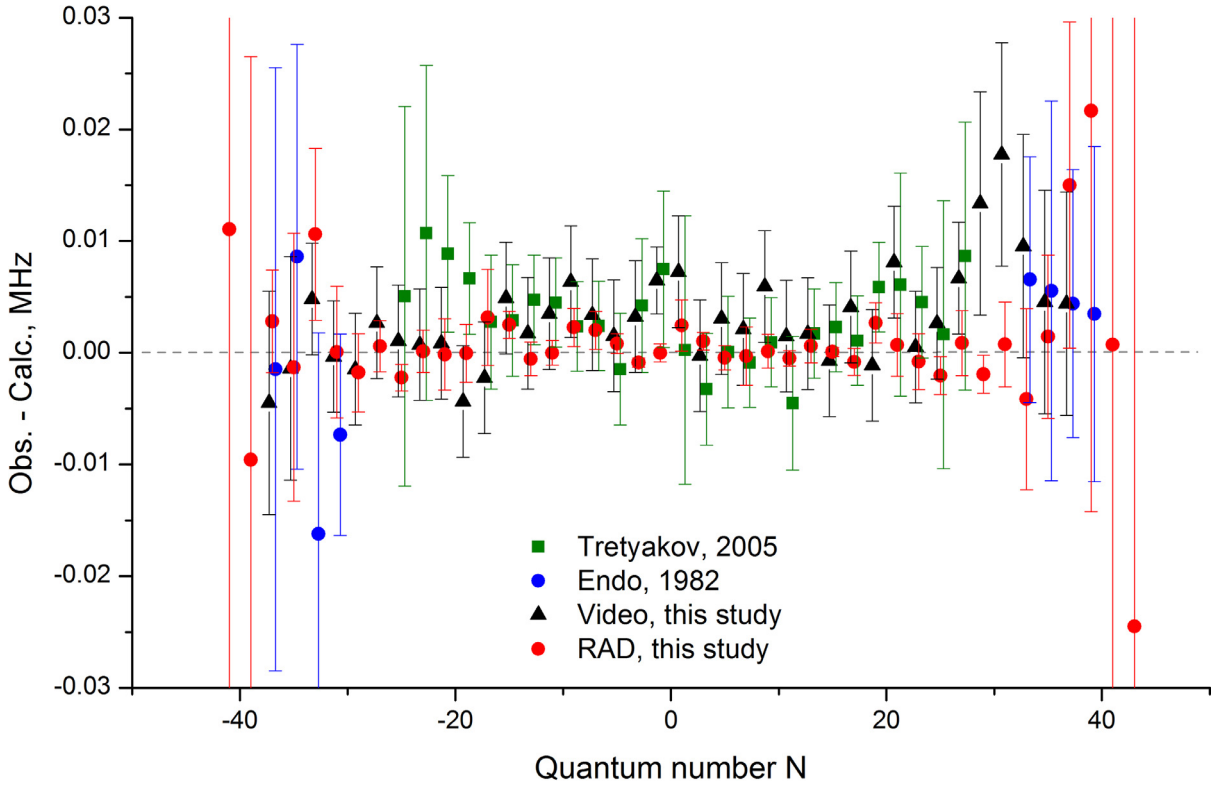

Fig. 7. Deviation of the experimental values from the calculated ones for independent sets of experimental data. For clarity, the datasets are slightly shifted relative to each other along the *X*-axis.

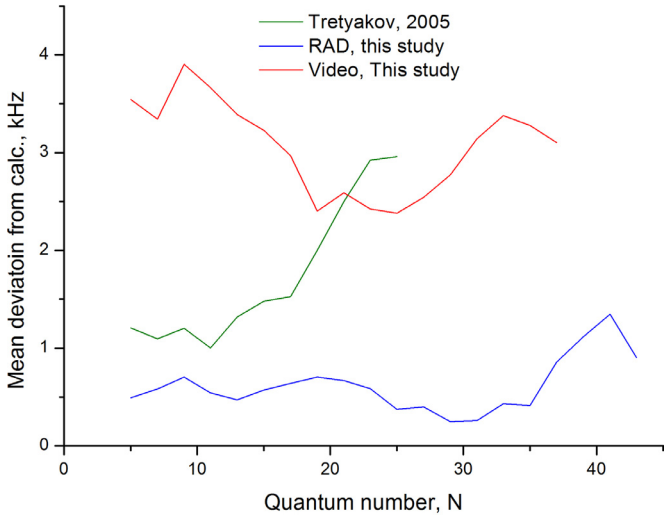

Fig. 8. Average deviation of experimental frequencies from the calculated values as a function of N_{max} for different datasets.

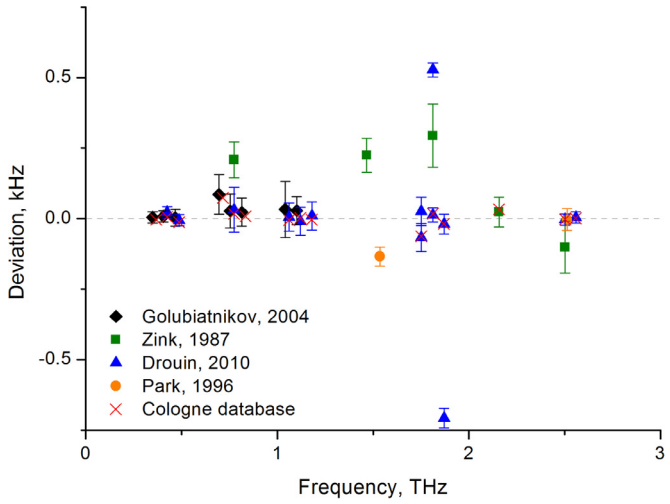

Fig. 9. The result of the rotational spectrum description with the refined fine structure spectrum. Different symbols correspond to deviations from the calculation for different measurement series (see legend). For comparison, the lines used in model optimization are marked with red crosses. The positions of the crosses correspond to the deviations from [33]. The different datasets are slightly shifted relative to each other along the *X*-axis for clarity.

of all 8 low-lying rotational transitions in the range from 0.34 to 1.1 THz (including the previously measured transition at 0.77 THz) using the RAD spectrometer are presented in [12]. The results of subsequent microwave measurements of the frequencies of 8 rotational transitions in the range from 0.47 to 1.87 THz, including repeated measurements of a number of lines and previously unmeasured lines near 1.18, 1.75, and 1.87 THz using video spectrometers in two different laboratories, are presented in [16]. The list of lines compiled as a result of the analysis of all these data, including the rejection of outliers and new unpublished data on microwave measurements of the lines at 2.5 and 2.55 THz, is the Cologne database [33]. This list of rotational lines is presented in Table 2 and is used in this work for an adequate comparison with the previous studies. Fig. 9 demonstrates the deviation of all the above experimental data on rotational transitions from the result of the simultaneous fit of the three above-mentioned sets of the fine-structure transition frequencies. In the same figure, crosses mark the deviations obtained when optimizing the complete set of data on the mi-

Table 2
Rotational transitions used in this work for data analysis in MHz.

Identification $N'_J - N_J$	Observed frequency	Obs.– Calc.	Calculated frequency
$3_2 - 1_1$	368,498.245(20)	0.0037	368,498.2414(73)
$3_2 - 1_2$	424,763.030(14)	0.0149	424,763.0151(72)
$3_3 - 1_2$	487,249.264(17)	−0.0032	487,249.2672(73)
$5_4 - 3_3$	715,392.980(70)	0.0852	715,392.8948(107)
$5_4 - 3_4$	773,839.512(48)	0.0289	773,839.4831(106)
$5_5 - 3_4$	834,145.560(50)	0.0222	834,145.5378(106)
$7_6 - 5_5$	1,061,123.830(50)	0.0051	1,061,123.8249(116)
$7_6 - 5_6$	1,120,714.821(31)	0.0132	1,120,714.8078(115)
$7_7 - 5_6$	1,179,879.019(50)	0.0093	1,179,879.0097(115)
$11_{10} - 9_9$	1,751,254.616(50)	−0.0676	1,751,254.6836(173)
$11_{10} - 9_{10}$	1,812,405.258(25)	0.0124	1,812,405.2457(173)
$11_{11} - 9_{10}$	1,870,017.709(35)	−0.0195	1,870,017.7285(173)
$13_{12} - 11_{12}$	2,157,577.773(52)	0.0230	2,157,577.7500(174)
$15_{14} - 13_{14}$	2,502,324.021(20)	−0.0038	2,502,324.0248(141)
$15_{15} - 13_{14}$	2,558,687.423(20)	0.0038	2,558,687.4192(141)

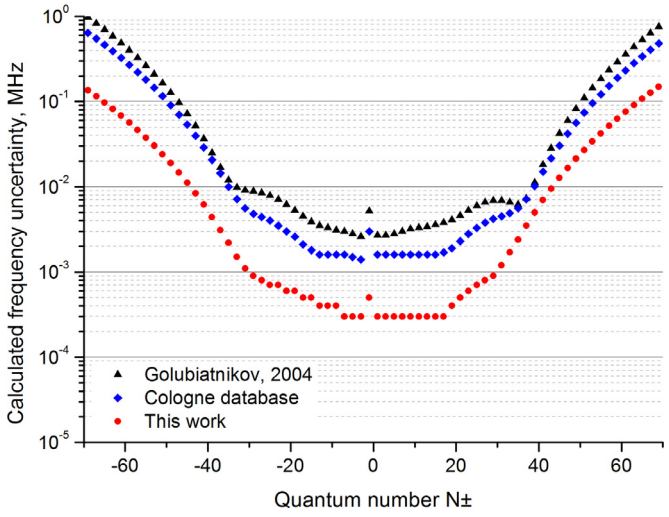

Fig. 10. Uncertainty of prediction of the fine structure frequencies of O_2 based on the results of various studies.

crowave spectrum of O_2 located in the Cologne database (including both fine structure lines and rotational ones).

Comparison of Figs. 9 and 7 makes it possible to conclude that the uncertainty of the frequencies of O_2 rotational transitions is more than an order of magnitude higher than the uncertainty of the fine structure frequencies. Therefore, even a significant increase in the accuracy of the latter has little effect on the description of the former. The RMS deviation of the frequencies of rotational transitions obtained in this paper is 31 kHz, which is about 3 kHz more than that obtained for the data [33]. Nevertheless, the change in the predictions of rotational frequencies, even for the most accurately measured lines of the first rotational triplet, does not go beyond the error bars and is negligible for all other transitions.

Thus, the performed analysis demonstrates the consistency of the three selected sets of experimental data for refining the description of the oxygen spectrum. The SPCAT [32] program is used to predict the spectrum frequencies and their uncertainties (Tables 1 and 2, right columns). Fig. 10 demonstrates the reduction of the uncertainty in predicting the frequencies of fine-structure transitions achieved in this work in comparison with the results of previous studies. The average relative increase in the prediction accuracy in the specified range of quantum numbers in comparison with the data [33] is about 4 times. For the fine-structure transitions included in modern models of radiation propagation in the atmosphere (up to $N = 29$), the prediction error is less than 1 kHz.

Table 3
Molecular constants of oxygen $^{16}O_2$ ($X^3\Sigma_g^-$, $v = 0$) in MHz.

Constant	Ref. [16]	This work
B_0	43,100.44276(88)	43,100.44183(83)
$D_0 \times 10^3$	145.1271(82)	145.1175(76)
$H_0 \times 10^9$	49(23)	24.9(191)
λ	59,501.3438(15)	59,501.34318(25)
$\lambda_D \times 10^3$	58.3680(97)	58.3549(20)
$\lambda_H \times 10^7$	2.908(90)	3.020(22)
γ	−252.58634(18)	−252.586504(39)
$\gamma_D \times 10^6$	−243.42(67)	−243.018(146)
$\gamma_H \times 10^9$	−1.46(46)	−1.555(111)
# lines	51	62

Note that the overwhelming part (86%) of the relative improvement in the description is provided by the dataset of the RAD spectrometer. The remaining 10% and 4% are added by the video spectrometer data and the joint dataset from [15] and [6], respectively.

The values of the spectroscopic constants obtained in this paper are shown in Table 3. For comparison, the constants obtained from the set [16] are also presented.

The uncertainty of the rotational constants has also slightly decreased by 3–6%. Their new values agree with the previous data within the error bars. The change in the fine structure constants turned out to be more significant. Their uncertainty has decreased by 4–6 times and for 3 of 6 constants the change exceeds the range of estimated uncertainty.

Summary

As a result of the study of the millimeter-wave spectrum of oxygen $^{16}O_2$ by two independent spectroscopic techniques, two sets of experimental frequencies of all fine structure lines in the ground state $X^3\Sigma_g^-$ are obtained up to $N = 43$. The statistical accuracy of the measured frequencies is several times higher than the accuracy of the previous data. The line shifting by pressure is taken into account, the estimate of the shifting and its rotational dependence is performed. The contribution of the effect is negligible for the video spectrometer, and is comparable to the value of the statistical error or exceeds it for the RAD spectrometer. Accounting for line shifting improves the agreement between the two datasets.

The obtained sets of experimental frequencies are used together with the results of previous measurements to refine the molecular constants of the ground state $X^3\Sigma_g^-$ of oxygen. As a result, the accuracy of determining the constants of the fine structure of oxygen increases several times in comparison with the most accurate previous studies [16]. For the fine structure transitions with N up to 29, included in modern models of atmospheric absorption, the un-

certainty of the transition frequencies prediction does not exceed 1 kHz. Also, as a result of our study, the uncertainty of extrapolation of dependences on lines with higher N has been reduced by several times. At the same time, the accuracy of describing the rotational spectrum of oxygen remains the same. Improvement of this accuracy is possible only by increasing the accuracy of determining the frequencies of the corresponding transitions and studying the higher rotational states.

Declaration of Competing Interest

The authors declare that they have no known competing financial interests or personal relationships that could have appeared to influence the work reported in this paper.

CRediT authorship contribution statement

M.A. Koshelev: Methodology, Investigation, Formal analysis, Writing – original draft, Writing – review & editing. **G.Yu. Golubiatnikov:** Investigation, Data curation, Writing – original draft. **I.N. Vilkov:** Investigation, Data curation. **M.Yu. Tretyakov:** Supervision, Conceptualization, Writing – original draft, Writing – review & editing.

Acknowledgments

The study was supported by a grant of the Russian Science Foundation (project No. 17-19-01602).

References

[1] Burkhalter JH, Anderson RS, Smith WV, Gordy W. The fine structure of the microwave absorption spectrum of oxygen. Phys Rev 1950;79(4):651–5.
[2] Zimmerer RW, Mizushima M. Precise measurement of the microwave absorption frequencies of the oxygen molecule and the velocity of light. Phys Rev 1961;121(1):152–5.
[3] McKnight JS, Gordy W. Measurement of the submillimeter-wave rotational transition of oxygen at 424 kMc/sec. Phys Rev Lett 1968;21:1787–9.
[4] Steinbach W, Gordy W. Pressure broadening of the rotational line of oxygen at 425GHz. Phys Rev A 1973;8:1753–8.
[5] Liebe HJ, Gimmestad GG, Hopponen JD. Atmospheric oxygen microwave spectrum experiment versus theory. IEEE Trans Antennas Propag 1977;AP-25(3):327–35.
[6] Endo Y, Mizushima M. Microwave resonance lines of $^{16}O_2$ in its electronic ground state ($X^3\Sigma_g^-$). Jpn J Appl Phys 1982;21:L379–80.
[7] Zink LR, Mizushima M. Pure rotational far-infrared transitions of $^{16}O_2$ in its electronic and vibrational ground state. J Mol Spectrosc 1987;125:154–8.
[8] Rouillé G, Millot G, Saint-Loup R, Berger H. High-resolution stimulated Raman spectroscopy of O_2. J Mol Spectrosc 1992;154:372–82.
[9] Park K, Nolt IG, Steele TC, Zink LR, Evenson KM, Chance KV, et al. Pressure broadening of the 50.873 cm^{-1} and the 83.469 cm^{-1} molecular oxygen lines. J Quant Spectrosc Radiat Transf 1996;56(2):315–16.
[10] Krupnov AF, Golubyatnikov GYu, Markov VN, Sergeev DA. Pressure broadening of the rotational line of oxygen at 425GHz. J Mol Spectrosc 2002;215:309–31.
[11] Brodersen S, Bendtsen J. The incoherent Raman spectrum of O-16(2) molecular constants from all experimental data. J Mol Spectrosc 2003;219:248–57.
[12] Golubyatnikov GYu, Krupnov AF. Microwave study of the rotational spectrum of oxygen molecule in the range up to 1.12 THz. J Mol Spectrosc 2003;217:282–7.
[13] Golubyatnikov GYu, Koshelev MA, Krupnov AF. Reinvestigation of pressure broadening parameters at 60-GHz band and single 118.75 GHz oxygen lines at room temperature. J Mol Spectrosc 2003;222:191–7.
[14] Golubyatnikov GYu, Krupnov AF. Molecular constants of the ground state of oxygen ($^{16}O_2$) accounting for new experimental data. J Mol Spectrosc 2004;225:222–4.
[15] Tretyakov MYu, Koshelev MA, Dorovskikh VV, Makarov DS, Rosenkranz PW. 60-GHz oxygen band: precise broadening and central frequencies of fine-structure lines, absolute absorption profile at atmospheric pressure, and revision of mixing coefficients. J Mol Spectrosc 2005;231:1–14.
[16] Drouin BJ, Yu S, Miller CE, Müller HSP, Lewen F, Brünken S, et al. Terahertz spectroscopy of oxygen, O2, in its $^3\Sigma_g^-$ and $^1\Delta$ electronic states: THz Spectroscopy of O_2. J Quant Spectrosc Radiat Transf 2010;111:1167–73.
[17] Meeks ML, Lilley AE. The microwave spectrum of oxygen in the Earth's atmosphere. J Geophys Res 1963;68(6):1683–703.
[18] Waters JW, Froidevaux L, Harwood RS, Jarnot RF, Pickett HM, et al. The Earth observing system microwave limb sounder (EOS MLS) on the Aura satellite. IEEE Trans Geosci Remote Sens 2006;44(5):1075–92.
[19] Wulfmeyer V, Hardesty RM, Turner DD, Behrendt A, Cadeddu MP, Girolamo PD, Schlüssel P, Van Baelen J, Zus F. A review of the remote sensing of lower tropospheric thermodynamic profiles and its indispensable role for the understanding and the simulation of water and energy cycles. Rev Geophys 2015;53:819–95. doi:10.1002/2014RG000476.
[20] Lawrence R, Lin B, Harrah S, Hu Y, Hunt P, Lipp C. Initial flight test results of differential absorption barometric radar for remote sensing of sea surface air pressure. J Quant Spectrosc Radiat Transf 2011;112:247–53.
[21] Leslie RV. NPOESS aircraft sounder testbed-microwave: observations of clouds and precipitation at 54, 118, 183, and 425 GHz. IEEE Trans Geosci Rem Sens 2004;42(10):2240–7.
[22] Rose T, Crewell S, Löhnert U, Simmer C(HATPRO). A network suitable microwave radiometer for operational monitoring of the cloudy atmosphere. Atmos Res 2005;75:183–200.
[23] Kulikov MYu, Krasil'nikov AA, Shvetsov AA, Fedoseev LI, et al. Simultaneous ground-based microwave measurements of the middle-atmosphere ozone and temperature. Radiophys Quant Electron 2015;58(6):409–17.
[24] Dicke RH. The effect of collisions upon the Doppler width of spectral line. Phys Rev 1953;89:472–3.
[25] Rautian SG. Universal asymptotic profile of a spectral line under a small Doppler broadening. Opt Spectrosc 2001;90(1):30–40.
[26] Konefał M, Kassi S, Mondelain D, Campargue A. High sensitivity spectroscopy of the O_2 band at 1.27 μm: (i) pure O_2 line parameters above 7920 cm^{-1}. J Quant Spectrosc Radiat Transf 2020;241:106653.
[27] Toureille M, Beguier S, Odintsova TA, Tretyakov MYu, Pirali O, Campargue A. The O_2 far-infrared absorption spectrum between 50 and 170 cm^{-1}. J Quant Spectrosc Radiat Transf 2020;242:106709.
[28] Tretyakov MYu, Koshelev MA, Makarov DS, Tonkov MV. Precise measurements of collision parameters of spectral lines with a spectrometer with radioacoustic detection of absorption in the millimeter and submillimeter ranges. Instrum Exp Tech+ 2008;51:78–88.
[29] Koshelev MA, Vilkov IN, Makarov DS, Tretyakov MYu, Rosenkranz PW. Speed-dependent broadening of the O_2 fine-structure lines. J Quant Spectrosc Radiat Transf 2021;264:107546.
[30] Koshelev MA, Golubiatnikov GYu, Vilkov IN, Tretyakov MYu. Line shape parameters of the 22-GHz water line for accurate modeling in atmospheric applications. J Quant Spectrosc Radiat Transf 2018;205:51–8.
[31] Golubiatnikov GYu, Belov SP, Leonov II, Andriyanov AF, Zinchenko II, Lapinov AV, et al. Precision sub-doppler millimeter and submillimeter lamb-dip spectrometer. Radiophys Quantum Electron 2014;56(8–9):599–609.
[32] Pickett HMthe JPL-program spfit.exe. J Mol Spectrosc 1991;148:371–7. Available from http://spec.jpl.nasa.gov/.
[33] https://cdms.astro.uni-koeln.de/classic/cologne_data (accessed August 23, 2021).
[34] Kochanov VP, Belov SP, Golubiatnikov GYu. Lamb dip spectroscopy with the use of frequency-modulated radiation. J Quant Spectrosc Radiat Transf 2014;149:146–57.
[35] Belov SP, Tretyakov MYu, Suenram RD. Improved laboratory rest frequency measurements and pressure shift and broadening parameters for the $J = 2 \leftarrow 1$ and $J = 3 \leftarrow 2$ rotational transitions of CO. Astrophys J 1992;393(2):848–51.
[36] Hartmann J-M, Boulet C, Robert D. Collisional effects on molecular spectra: laboratory experiments and models, consequences for applications. Elsevier Science; 2008.
[37] Townes CH, Schawlow AL. Microwave spectroscopy. Dover Publications; 1975. ISBN 9780486617985.